

K. KOWALCZYK-GAJEWSKA*, S. STUPKIEWICZ*

MODELLING OF TEXTURE EVOLUTION IN KOBO EXTRUSION PROCESS**MODELOWANIE ROZWOJU TEKSTURY W PROCESIE WYCISKANIA METODĄ KOBO**

The paper is aimed at modelling of evolution of crystallographic texture in KOBO extrusion which is an unconventional process of extrusion assisted by cyclic torsion. The analysis comprises two steps. In the first step, the kinematics of the KOBO extrusion process is determined using the finite element method. A simplifying assumption is adopted that the material flow is not significantly affected by plastic hardening, and thus a rigid-viscoplastic material model with no hardening is used. In the second step, evolution of crystallographic texture is modelled along the trajectories obtained in the first step. A micromechanical model of texture evolution is used that combines the crystal plasticity model with a self-consistent grain-to-polycrystal scale transition scheme, and the VPSC code is used for that purpose. Since each trajectory corresponds to a different deformation path, the resulting pole figures depend on the position along the radius of the extruded rod.

Keywords: plasticity, microstructure, crystallographic texture, KOBO extrusion

Praca jest poświęcona modelowaniu rozwoju tekstury krystalograficznej w procesie wyciskania metodą KOBO – niekonwencjonalnym procesie wyciskania przy udziale cyklicznego skręcania. Analiza jest prowadzona w dwóch krokach. W pierwszym kroku, przy pomocy metody elementów skończonych, wyznaczane jest pole deformacji w procesie KOBO przy upraszczającym założeniu, że nie zależy ono w sposób istotny od umocnienia materiału. W pracy zastosowano model sztywno-lepkoplastyczny bez umocnienia. W drugim kroku, modelowany jest rozwój tekstury krystalograficznej wzdłuż trajektorii wyznaczonych w pierwszym kroku. W tym celu wykorzystano mikromechaniczny model łączący model plastyczności kryształów i samoczynny schemat przejścia mikro-makro zaimplementowany w programie VPSC. Ponieważ ścieżka deformacji jest inna dla każdej trajektorii, wynikowe figury biegunowe wykazują zależność od położenia wzdłuż promienia wyciskanego pręta

1. Introduction

Metals subjected to large plastic deformations undergo substantial changes of microstructure, and their macroscopic properties are governed by the associated effects such as formation of dislocation structures, grain refinement, texture development, and others. During last decades, there has been a significant progress in characterization and physical understanding of these phenomena. Modelling of microstructural evolution during plastic deformation has also been an area of active research; however, complete models of the related phenomena are still missing.

Modelling of evolution of crystallographic texture is a well-established topic. The corresponding models combine constitutive equations for a single crystal with a grain-to-polycrystal scale transition scheme. The former models are typically developed in the framework of crystal plasticity theory [1, 2] which is particularly suitable for describing plastic deformation at the micro-scale, as it considers activity of individual slip systems in a crystal. Crystal plasticity models of texture evolution proved highly successful in the applications related to metal forming processes [3, 4, 5], considering

various effects such as the elongated or flattened grain shape and grain interactions [6, 7, 8, 9], nonuniform evolution of dislocation density [10], twinning [11, 12, 13, 14], and others. It has been concluded that the Taylor model delivers acceptable results for high symmetry crystals and monotonic strain paths, while it fails for low symmetry crystals and processes involving strain path changes. The self-consistent model provides then better predictions, e.g., [15, 16].

Severe plastic deformation (SPD) processes, such as equal channel angular pressing (ECAP) [17], are designed to intentionally impose very large plastic strains with the aim to refine the grain structure to submicron size [18]. The SPD processes lead also to substantial texture changes which have a significant impact on post-processed material behavior including, above all, plastic anisotropy but also strength, work hardening, formability and fracture. These structural properties of interest cannot be fully understood without proper characterization of texture evolution in the considered SPD processes. However, in these processes, the material is subjected to complex strain paths, and the texture evolution models seem less successful in predicting the final textures [16]. The plausible reason is

* INSTITUTE OF FUNDAMENTAL TECHNOLOGICAL RESEARCH (IPPT), 02-106 WARSAW, 5B PAWIŃSKIEGO STR., POLAND

that grain refinement and its interaction with texture evolution is still not adequately modelled.

In fact, despite significant research efforts, modelling of grain refinement during plastic deformation is still at an early stage. On one hand, microstructure formation is studied at the single crystal scale using an energy minimization approach [19, 20, 21], and the reasons for inhomogeneity or deformation banding of multi-slip plastic flow are sought, for instance, in a proper formulation of the crystal plasticity model combined with an energy criterion [22, 23]. But these models are still far from being applicable to the actual forming or SPD processes. On the other hand, phenomenological models are developed which provide quantitative description of evolution of selected microstructure parameters without referring to the details of plastic deformation at the micro-scale, e.g., [24]. The latter model has been used to simulate microstructure evolution and grain refinement in several SPD processes [24, 25, 26], as well as in a complex forming process of KOB0 extrusion [27].

The KOB0 extrusion process, which is studied in this work, is a non-conventional process of extrusion assisted by cyclic rotation of the die [28, 29]. Its technological advantages include substantial reduction of extrusion force, ultra-fine grain structure of the product, and others, cf. [30]. At the same time, only few published results on modelling of this process are available [27, 31, 32]. In reference to the KOB0 extrusion process, modelling of texture evolution has only been performed for an idealized process of tension or compression assisted by cyclic torsion [33], in which the strain path is, however, significantly different than in the actual KOB0 extrusion process.

In this work, the general approach proposed in [27] in the context of modelling of grain refinement is applied to modelling of texture evolution in KOB0 extrusion. Following the approach of [27], the analysis comprises two steps. In the first step, the kinematics of the KOB0 extrusion process is determined for a non-hardening material using the finite element method. This part is briefly described in Section 2. In the second step of analysis, evolution of crystallographic texture is predicted along the deformation paths determined in the first step. The micromechanical model [15] used for that purpose is presented in Section 3. The model combines the rate-dependent crystal plasticity model and the self-consistent grain-to-polycrystal transition scheme. The VPSC code [15] is employed in the actual computations. The results are presented and discussed in Section 4. For completeness, the predictions of the classical Taylor model are also included.

2. Kinematics of KOB0 extrusion process

The principle of the KOB0 extrusion process [28, 29] is illustrated in Fig. 1. The complex kinematics of the KOB0 extrusion process is determined here using the approach proposed in [27]. The effect of material hardening on the kinematics of the process is neglected at this stage. Under this assumption, the solution of the problem of axisymmetric extrusion with cyclic torsion can be constructed in terms of the solution of steady-state extrusion with torsion, as described below.

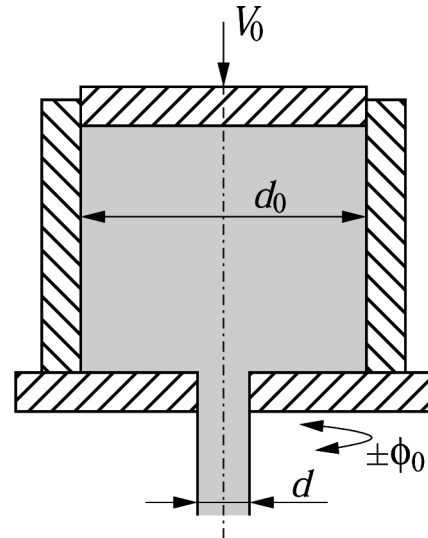


Fig. 1. Scheme of the KOB0 extrusion process: extrusion assisted by cyclic rotation of the die

In the steady-state axisymmetric extrusion with torsion, the billet is extruded with a constant axial velocity V_0 , and the die rotates with a constant angular velocity Ω_0 . Variation of the billet height is neglected. The velocity field is specified by three unknown fields, namely the radial velocity $v_r(r, z)$, the axial velocity $v_z(r, z)$, and the angular velocity $\omega(r, z)$ such that $v_\phi = r\omega(r, z)$ is the circumferential velocity. As the unknown fields depend only on the cylindrical coordinates r and z , the problem is two-dimensional.

Constitutive equations are specified by the rigid-viscoplastic Norton-Hoff model that relates σ' , the deviatoric part of the Cauchy stress tensor σ , and \mathbf{d} , the Eulerian strain-rate tensor,

$$\sigma' = \frac{2}{3} \frac{\sigma_y}{d_{II}^0} \left(\frac{d_{II}}{d_{II}^0} \right)^{m-1} \mathbf{d}, \quad d_{II} = \sqrt{\frac{2}{3} \mathbf{d} \cdot \mathbf{d}}. \quad (1)$$

Here, σ_y is the reference yield stress, d_{II}^0 is the reference strain-rate, and $0 < m < 1$ is the strain-rate sensitivity coefficient. In view of incompressibility, we have $\text{tr} \mathbf{d} = 0$.

The problem of steady-state extrusion with torsion is solved using the finite element method. The simplified geometry shown in Fig. 1 is adopted with the following boundary conditions. Constant velocity is prescribed at the top surface ($v_z = V_0, v_r = 0, \omega = 0$), and sticking contact is assumed along the rotating die at the bottom of the container ($v_z = v_r = 0, \omega = \Omega_0$). Bilateral contact ($v_r = 0$) is enforced along the container wall ($r = d_0/2$) and die exit ($r = d/2$), and friction is assumed along the container wall in the form of the Tresca model with viscous regularization similar to that in the Norton-Hoff model (1). The standard details of finite-element formulation and implementation are omitted here. The computations have been carried out using the *AceGen/AceFEM* system (<http://www.fgg.uni-lj.si/symech/>).

Having the solution for the steady-state extrusion problem with torsion, the time-dependent solution for the extrusion problem with cyclic torsion is constructed by simply changing the sign of the angular velocity in a cyclic manner, $\omega^*(r, z, t) = \pm\omega(r, z)$, while the radial and axial velocities are constant in time, $v_r^*(r, z, t) = v_r(r, z)$ and $v_z^*(r, z, t) = v_z(r, z)$.

This scheme is exact for a piecewise constant angular velocity of the die $\pm\Omega_0$. In the case of the Norton-Hoff model, the flow stress is not sensitive to prior history, so that all the governing equations are satisfied at each time instant. For a harmonic oscillation of the die, the above solution scheme can be directly applied for the case of constant extrusion force with an approximation due minor viscous effects being neglected.

It has been shown in [27] that the effect of cyclic rotation of the die on the flow pattern observed in experiments [29] is correctly reproduced by the proposed computational scheme. The characteristic radial flow with superimposed cyclic changes of the trajectory is illustrated in Fig. 2 which shows three-dimensional trajectories of the material points initially located at $r_0 = 2, 6, 10, 14, 18$ mm. It is seen that the actual deformation zone is confined to the vicinity of the die. The trajectories in Fig. 2a are computed for the KOBO extrusion process analyzed in Section 4. In Fig. 2b, the torsion angle has been increased and the frequency has been reduced by the factor of four so that the zigzag motion along the radial path is seen more clearly, while the reference problem of steady-state extrusion with torsion is the same.

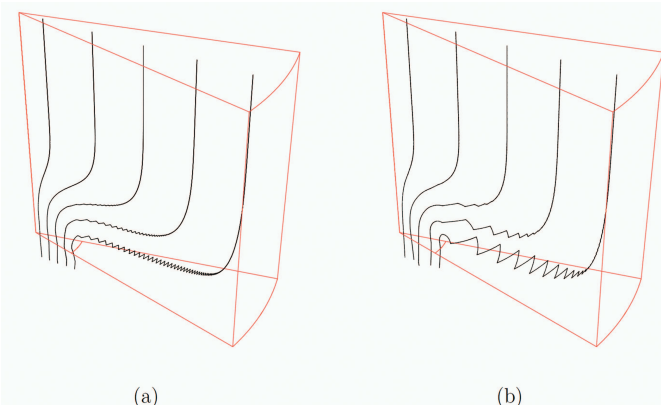


Fig. 2. Three-dimensional trajectories of selected points ($r_0 = 2, 6, 10, 14, 18$ mm) during KOBO extrusion: (a) $\phi_0 = 4^\circ$, $f = 8$ Hz, (b) $\phi_0 = 16^\circ$, $f = 2$ Hz (the remaining process parameters are specified in Section 4). The red lines indicate a slice of the billet, and the small red circular arc at the bottom indicates the die exit

3. Crystal-plasticity model of texture evolution

The texture evolution model used in this work combines the crystal plasticity model with the self-consistent grain-to-polycrystal scale transition scheme. The two ingredients are briefly introduced in this section, and the details can be found in [3, 15].

The large strain formulation of the crystal plasticity theory is applied [3]. The assumption is made that the elastic stretches are negligible compared to the plastic strains so that the elastic part is restricted to a rigid rotation. Consequently, the additive decomposition of the total velocity gradient \mathbf{L} into the elastic spin $\mathbf{\Omega}^*$ and the plastic part \mathbf{L}^p is obtained,

$$\mathbf{L} = \mathbf{\Omega}^* + \mathbf{L}^p. \quad (2)$$

It is common for crystal plasticity models to assume that during the elastic regime the crystallographic lattice and the

material undergo the same deformation while the plastic flow does not induce any lattice rotation. The evolution of the lattice orientation, described by rotation \mathbf{R} , is thus governed by the following relation:

$$\dot{\mathbf{R}} = \mathbf{\Omega}^* \mathbf{R} = (\mathbf{\Omega} - \mathbf{\Omega}^p) \mathbf{R}, \quad (3)$$

where $\mathbf{\Omega}$ and $\mathbf{\Omega}^p$ are skew-symmetric parts of \mathbf{L} and \mathbf{L}^p , respectively.

Plastic deformation occurs by slip in a crystallographic direction \mathbf{m}^r on a crystallographic plane with a unit normal \mathbf{n}^r , $r = 1, \dots, M$, where M is the number of slip systems. The plastic part of the velocity gradient is then specified as follows:

$$\mathbf{L}^p = \sum_{r=1}^M \dot{\gamma}^r \mathbf{m}^r \otimes \mathbf{n}^r. \quad (4)$$

In this work, the slip systems relevant for the fcc materials are considered, i.e. there are twelve slip systems of the $\{111\}\langle 110 \rangle$ type.

The constitutive equation relates the resolved shear stress $\tau^r = \mathbf{n}^r \cdot \boldsymbol{\sigma} \cdot \mathbf{m}^r$, where $\boldsymbol{\sigma}$ is the Cauchy stress tensor, with the slip rate $\dot{\gamma}^r$ according to the viscoplastic power law [3],

$$\dot{\gamma}^r = \dot{\gamma}_0 \text{sign}(\tau^r) \left| \frac{\tau^r}{\tau_c^r} \right|^n. \quad (5)$$

It is assumed that the critical shear stress τ_c^r evolves according to the following hardening law [34],

$$\dot{\tau}_c^r = h_0 \left(1 - \frac{\tau_c^r}{\tau_{sat}^r} \right)^\beta \sum_{q=1}^M h_{rq} |\dot{\gamma}^q|, \quad h_{rq} = q + (1 - q) |\mathbf{n}^r \cdot \mathbf{n}^q|. \quad (6)$$

The above form of the hardening matrix h_{rq} accounts for the difference between the latent hardening for coplanar and non-coplanar slip systems. The material parameters take values applicable to copper [35], i.e. $\tau_c^0 = 14$ MPa, $h_0 = 232.75$ MPa, $\tau_{sat} = 138.6$ MPa, $\beta = 2.5$, $q = 1.6$, $n = 20$, $\dot{\gamma}_0 = 10^{-3}$ 1/s.

The response of a polycrystalline aggregate is obtained by averaging the responses of individual grains in the representative volume element (RVE), the local response being governed by the constitutive equations described above. As mentioned in the Introduction, the visco-plastic self-consistent (VPSC) scheme [15] is known to deliver reliable results, and this scheme is used in the present work. As a reference, the results corresponding to the simple Taylor scheme are also provided.

A grain aggregate composed of $N = 500$ grains of equal volume fractions is considered as a RVE. Initially, the grains within the aggregate have the same equiaxed shape and random distribution of lattice orientations. The macroscopic velocity gradient $\bar{\mathbf{L}}$ and the macroscopic stress tensor $\bar{\boldsymbol{\Sigma}}$ in the aggregate are specified as

$$\bar{\mathbf{L}} = \frac{1}{N} \sum_{g=1}^N \mathbf{L}^g, \quad \bar{\boldsymbol{\Sigma}} = \frac{1}{N} \sum_{g=1}^N \boldsymbol{\sigma}^g. \quad (7)$$

In the Taylor averaging scheme, all grains in the aggregate share the same velocity gradient, viz.

$$\mathbf{L}^g = \bar{\mathbf{L}}. \quad (8)$$

In the VPSC scheme, a single grain is treated as an inclusion in the effective medium of equivalent averaged properties of the aggregate, so that the local strain rate and stress tensors are related to the macroscopic quantities by the interaction equation of the form [36]

$$\sigma^g - \Sigma = -\mathbf{L}^* \cdot (\mathbf{d}^g - \mathbf{D}), \quad (9)$$

where the Hill tensor \mathbf{L}^* depends on the shape of the inclusion and on the averaged properties of the aggregate, while \mathbf{d}^g and \mathbf{D} denote, respectively, the local and the macroscopic strain rate tensors defined as symmetric parts of the corresponding velocity gradients.

The self-consistent scheme relies on the Eshelby solution to the inhomogeneity problem obtained for a linear constitutive equation. Its application in the case of non-linear viscoplasticity requires the material response to be linearized at each time increment. Different ways of linearization have been proposed in the literature. In this work, we use the affine self-consistent model as discussed in [37].

4. Results

To simulate the texture evolution in the KOBO extrusion process, the grain aggregate is subjected to the strain paths determined using the procedure described in Section 2 for the following parameters of the KOBO extrusion process: diameter reduction $d_0 : d = 40 : 8$ mm, die rotation angle $\phi_0 = 4^\circ$, die rotation frequency $f = 8$ Hz, and extrusion velocity $V_0 = 1$ mm/s. The results are presented for sample strain paths corresponding to the material points initially located at $r_0 = 0, 6, 12, 15, 18$ mm (the corresponding final radii are $r = 0, 1.2, 2.4, 3.0, 3.6$ mm, respectively).

The $\{111\}$ pole figures presenting the final texture obtained for the Taylor model and the self-consistent (VPSC) model are shown in Fig. 3. Two ways of presentation of the results are used: discrete point plots showing the orientation of each $\{111\}$ pole for each of 500 grains and contour plots presenting the reconstructed orientation distribution functions for the same set of data. In both cases, the extrusion (axial) direction is perpendicular to the figure, and the radial direction is aligned with the horizontal axis of the figure. It is seen that the texture evolution within the extruded element is strongly heterogeneous depending on the location of the material point within the cross-section. In the center ($r_0 = 0$), the texture image is equivalent to the one resulting from the classical extrusion process because the torsion affects only the material points outside the symmetry axis. For $r_0 > 0$, the texture loses its axial symmetry, and it exhibits the symmetry only with respect to the horizontal axis. In the material elements subjected to severe cyclic torsion (Fig. 3c-d), strong texture develops characterized by the presence of intensive poles corresponding to specific orientations of crystallites.

Figure 4 shows the inverse pole figures for the final texture presenting orientation of the extrusion axis with respect the crystal axes. Due to the cubic crystal symmetry, only the basic triangle is shown. Again, for the material points located at the center of the extruded cylinder, the texture corresponds to the classical result for the extrusion process: the extrusion

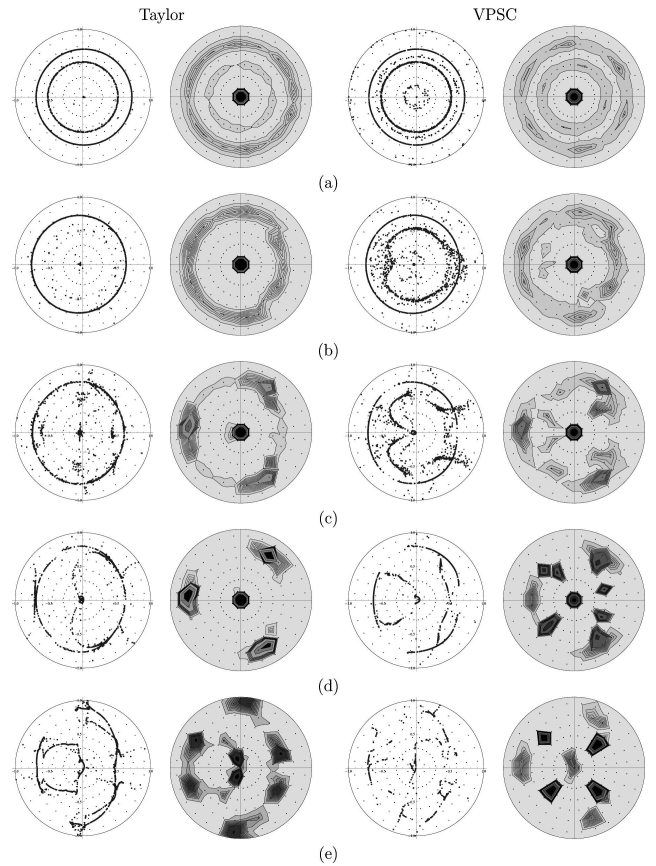


Fig. 3. $\{111\}$ pole figures after KOBO-extrusion process: (a) $r = 0$, (b) $r = 1.2$ mm, (c) $r = 2.4$ mm, (d) $r = 3.0$ mm, (e) $r = 3.6$ mm

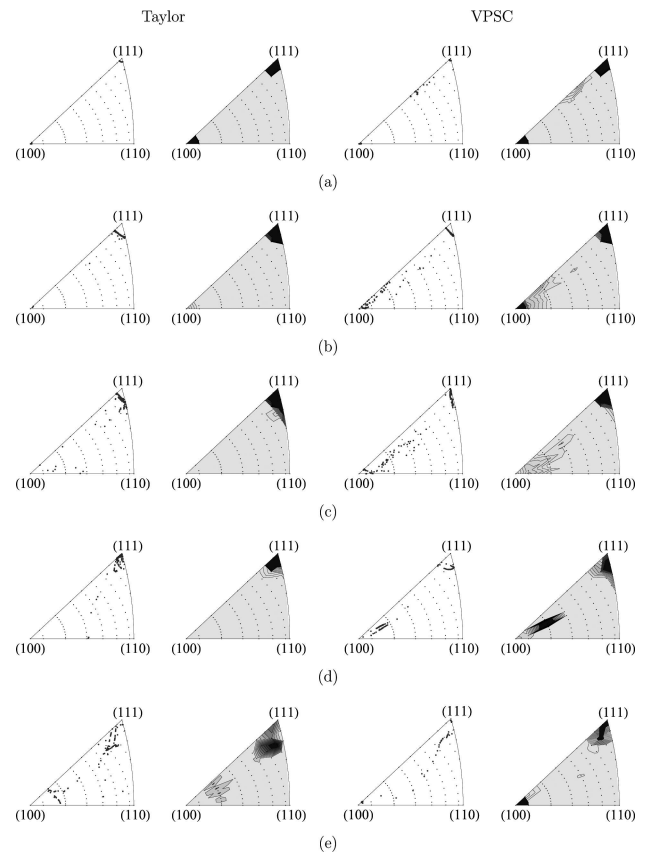


Fig. 4. $[001]$ inverse pole figures after KOBO-extrusion process: (a) $r = 0$, (b) $r = 1.2$ mm, (c) $r = 2.4$ mm, (d) $r = 3.0$ mm, (e) $r = 3.6$ mm

axis is coaxial with the $\langle 111 \rangle$ crystallographic directions in most of the crystallites, and it is coaxial with the $\langle 100 \rangle$ directions for a small fraction of the crystallites. As the contribution of cyclic torsion increases with increasing radius, the orientation of extrusion axis with respect to the crystal frame deviates and additional orientations appear. However, there is always an important fraction of crystallites for which the extrusion axis is close to the $\langle 111 \rangle$ directions. The difference in the predictions of the Taylor model and the VPSC model is clearly seen, especially concerning the fraction of crystallites with extrusion axis close to the $\langle 100 \rangle$ crystal axis.

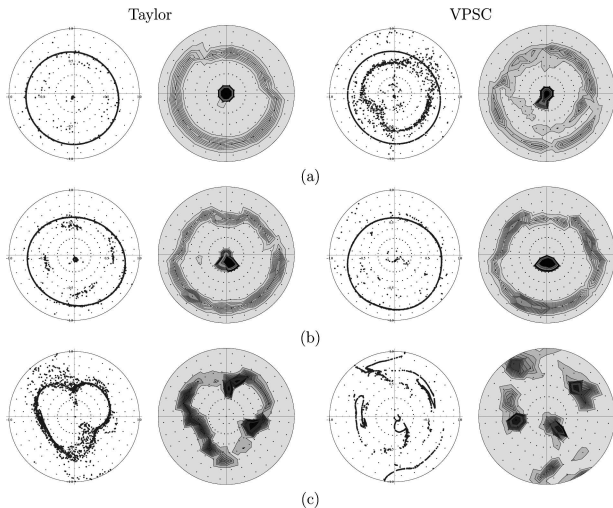


Fig. 5. $\{111\}$ pole figures after extrusion process assisted by monotonic torsion: (a) $r = 1.2$ mm, (b) $r = 2.4$ mm, (c) $r = 3.6$ mm

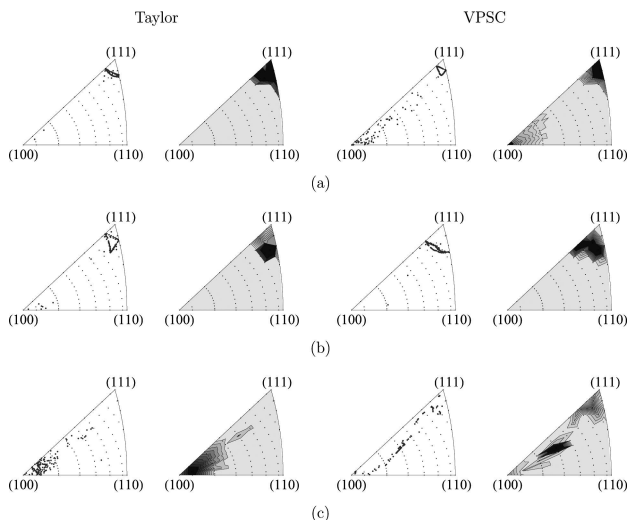


Fig. 6. $[001]$ inverse pole figures after extrusion process assisted by monotonic torsion: (a) $r = 1.2$ mm, (b) $r = 2.4$ mm, (c) $r = 3.6$ mm

The influence of the cyclic character of the die rotation on the texture evolution has been also studied. To this end, the texture evolution has been simulated for a hypothetical extrusion process assisted by a monotonic rotation of the die. The results are presented in Figs. 5 and 6. It is seen that the pole figures lose their symmetry as compared to the cyclic process. Similarly to the cyclic process, in the case of intensive shearing deformation far from the extrusion axis, intensive

poles are obtained, especially for the textures simulated using the VPSC model.

In the available literature, the experimental data concerning texture development in the KOBO extrusion process are scarce. In [38], experimental textures are reported for the Mg-based AZ alloy (hcp metal) subjected to KOBO extrusion. As concerns the fcc metals, we are only aware of the conference communication [39] focusing on the KOBO-extruded copper. It has been reported in [39] that the typical extrusion fiber texture is formed in the center of the extruded rod, while single blocks of orientations are observed in the regions of intensive plastic flow assisted by torsion. Qualitatively, these features are reproduced by the present modelling. However, a quantitative comparison is not possible due to the lack of respective experimental data.

5. Conclusion

A modelling approach has been proposed for prediction of texture development in KOBO extrusion – an unconventional process of extrusion assisted by cyclic torsion of the die. The deformation field and the trajectories of material points have been determined for a non-hardening material using the finite element method. Subsequently, evolution of crystallographic texture has been modelled along these trajectories. A micro-mechanical model combining the crystal plasticity model and the self-consistent grain-to-polycrystal scale transition scheme has been used for that purpose. For comparison, predictions of the classical Taylor averaging scheme have also been computed.

The resulting pole figures depend on the position along the radius of the extruded rod. This is because each trajectory corresponds to a substantially different deformation path. As the crystallographic texture is the source of plastic anisotropy, non-uniform texture is expected to result in strong heterogeneity of plastic properties within the rod.

The presented results confirm that the grain-to-polycrystal scale transition scheme has a significant influence on the texture image predicted by the model. Based on the results reported for other forming processes, e.g., for ECAP [16], it is expected that the predictions of the affine VPSC scheme are more reliable than those of the Taylor scheme. Nevertheless experimental validation of the present predictions is necessary and would be an interesting subject of future research.

Acknowledgements

This work has been supported by the Polish Ministry of Science and Higher Education through the KomCerMet project (contract no. POIG.01.03.01-00- 013/08) in the framework of the Operational Programme Innovative Economy 2007-2013.

REFERENCES

- [1] R. Hill, and J.R. Rice, Constitutive analysis of elastic-plastic crystals at arbitrary strain. *J. Mech. Phys. Solids* **20**, 401-413 (1972).
- [2] R.J. Asaro, Micromechanics of crystals and polycrystals. *Adv. Appl. Mech.* **23**, 1-115 (1983).

- [3] R.J. Asaro, and A. Needleman, Texture development and strain hardening in rate dependent polycrystals. *Acta metall.* **33**(6), 923-953 (1985).
- [4] S.R. Kalidindi, and L. Anand, Macroscopic shape change and evolution of crystallographic texture in pre-textured fcc metals. *J. Mech. Phys. Solids* **42**, 459-490 (1994).
- [5] K. Kowalczyk, and W. Gambin, Model of plastic anisotropy evolution with texture – dependent yield surface. *Int. J. Plasticity* **20**, 19-54 (2004).
- [6] P. Van Houtte, On the equivalence of the relaxed Taylor theory and the Bishop-Hill theory for partially constrained plastic deformation of crystal. *Mater. Sci. Eng.* **55**, 69-77 (1982).
- [7] T. Leffers, and D. Juul Jensen, The relation between texture and microstructure in rolled fcc materials. *Text. Microstruct.* **14-18**, 933-952 (1991).
- [8] P. Van Houtte, S. Li, M. Seefeldt, and L. Delannay, Deformation texture prediction: from the Taylor model to the advanced Lamel model. *Int. J. Plasticity* **21**, 589-624 (2005).
- [9] K. Kowalczyk-Gajewska, Micromechanical modelling of metals and alloys of high specific strength. *Prace IPPT 1/2011*, Warszawa 2011.
- [10] Y. Estrin, L.S. Toth, A. Molinari, and Y. Bréchet, A dislocation-based model for all hardening stages in large strain deformation. *Acta mater.* **46**, 5509-5522 (1998).
- [11] P. Van Houtte, Simulation of the rolling texture and shear texture of brass by the Taylor theory adapted for mechanical twinning. *Acta Metal.* **26**, 591-604 (1978).
- [12] C.N. Tomé, R. A. Lebensohn, and U.F. Kocks, A model for texture development dominated by deformation twinning: application to zirconium alloy. *Acta Metal. Mater.* **39**, 2667-2680 (1991).
- [13] G. Proust, C.N. Tomé, and G.C. Kaschner, Modeling texture, twinning and hardening evolution during deformation of hexagonal materials. *Acta Mater.* **55**, 2137-2148 (2007).
- [14] K. Kowalczyk-Gajewska, Modelling of texture evolution in metals accounting for lattice reorientation due to twinning. *Eur. J. Mech. Solids/A* **29**, 28-41 (2010).
- [15] R.A. Lebensohn, and C.N. Tomé, A self-consistent anisotropic approach for the simulation of plastic deformation and texture development of polycrystals: Application to zirconium alloys. *Acta Metall. Mater.* **41**, 2611-2624 (1993).
- [16] I.J. Beyerlein, and L.S. Toth, Texture evolution in equal-channel angular extrusion. *Progress Mater. Sci.* **54**, 427-510 (2009).
- [17] V.M. Segal, Materials processing by simple shear. *Mater. Sci. Eng. A* **197**, 157-164 (1995).
- [18] R.Z. Valiev, and T.G. Langdon, Principles of equal-channel angular pressing as a processing tool for grain refinement. *Progress Mater. Sci.* **51**, 881-981 (2006).
- [19] M. Ortiz, and E.A. Repetto, Nonconvex energy minimization and dislocation structures in ductile single crystals. *J. Mech. Phys. Solids* **47**, 397-462 (1999).
- [20] C. Miehe, M. Lambrecht, and E. Gurses, Analysis of material instabilities in inelastic solids by incremental energy minimization and relaxation methods: evolving deformation microstructures in finite plasticity. *J. Mech. Phys. Solids* **52**, 2725-2769 (2004).
- [21] D.M. Kochmann, and K. Hackl, The evolution of laminates in finite crystal plasticity: a variational approach. *Continuum Mech. Thermodyn.* **23**, 63-85 (2011).
- [22] H. Petryk, and M. Kurza, Selective symmetrization of the slip-system interaction matrix in crystal plasticity. *Arch. Mech.* **63**, 287-310 (2011).
- [23] H. Petryk, and M. Kurza, The energy criterion for deformation banding in ductile single crystals. *J. Mech. Phys. Solids* (2013), Submitted.
- [24] H. Petryk, and S. Stupkiewicz, A quantitative model of grain refinement and strain hardening during severe plastic deformation. *Mater. Sci. Eng. A* **444**, 214-219 (2007).
- [25] M. Richert, H. Petryk, and S. Stupkiewicz, Grain refinement in AlMgSi alloy during cyclic extrusion-compression: experiment and modelling. *Arch. Metall. Mater.* **52**(1), 49-54 (2007).
- [26] H. Petryk, S. Stupkiewicz, and R. Kuziak, Grain refinement and strain hardening in IF steel during multi-axis compression: Experiment and modelling. *J. Mat. Proc. Technol.* **204**, 255-263 (2008).
- [27] H. Petryk, and S. Stupkiewicz, Modelling of microstructure evolution on complex paths of large plastic deformation. *Int. J. Mat. Res.* **103**, 271-277 (2012).
- [28] A. Korbel, and W. Bochniak, The structure based design of metal forming operations. *J. Mat. Proc. Technol.* **53**, 229-237 (1995).
- [29] W. Bochniak, and A. Korbel, Plastic flow of aluminium extruded under complex conditions. *Mater. Sci. Technol.* **16**, 664-669 (2000).
- [30] W. Bochniak, K. Marszowski, and A. Korbel, Theoretical and practical aspects of the production of thin-walled tubes by the KOBO method. *J. Mat. Proc. Technol.* **169**, 44-53 (2005).
- [31] A. Żmudzki, W. Wajda, H. Paul, and M. Pietrzyk, Assessment of energy balance in the extrusion process characterized by strain path change induced by deformation. *Rudy Metale* **51**, 260-266 (2006). (in Polish).
- [32] J. Maciejewski, and Z. Mróz, An upper-bound analysis of axisymmetric extrusion assisted by cyclic torsion. *J. Mat. Proc. Technol.* **206**, 333-344 (2008).
- [33] K. Kowalczyk-Gajewska, Z. Mróz, and R.B. Pęcherski, Micromechanical modelling of polycrystalline materials under non-proportional deformation paths. *Arch. Metall. Mater.* **52**, 181-192 (2007).
- [34] L. Anand, Single-crystal elasto-viscoplasticity: application to texture evolution in polycrystalline metals at large strain. *Comput. Methods Appl. Mech. Engrg.* **193**, 5359-5383 (2004).
- [35] K. Kowalczyk-Gajewska, and R.B. Pęcherski, Phenomenological description of the effect of micro-shear banding in micromechanical modelling of polycrystal plasticity. *Arch. Metall. Mater.* **54**, 1145-1156 (2009).
- [36] A. Molinari, G.R. Canova, and S. Ahzi, Self-consistent approach of the large deformation polycrystal visco-plasticity. *Acta Metall.* **35**, 2983-2994 (1987).
- [37] R. Masson, M. Bornert, P. Suquet, and A. Zaoui, An affine formulation for the prediction of the effective properties of non-linear composites and polycrystals. *J. Mech. Phys. Solids* **48**, 1203-1227 (2000).
- [38] J. Pospiech, A. Korbel, J. Bonarski, W. Bochniak, and L. Tarkowski, Microstructure and texture of Mg-based AZ alloys after heavy deformation under cyclic strain path change conditions. *Mater. Sci. Forum* **584-586**, 565-570 (2008).
- [39] A. Korbel, L. Błaż, F. Stalony-Dobrzański, J. Bonarski, L. Tarkowski, and J. Pospiech, Characterization methods for metallic materials deformed in the large strain regime (in Polish). Presented at *PlastMet VI Seminar*, Łańcut 2008.